

# Autoionization of Homogeneous Nickel(II) Diphosphane Hydrogenation Catalysts. An NMR Study and Crystal Structures of $[\text{Ni}(o\text{-MeO-dppe})\text{I}_2]$ and $[\text{Ni}(o\text{-MeO-dppe})_2](\text{PF}_6)_2$

Ingrid M. Angulo,<sup>†</sup> Elisabeth Bouwman,<sup>\*,†</sup> Martin Lutz,<sup>‡</sup> Wilhelmus P. Mul,<sup>\*,§</sup> and Anthony L. Spek<sup>‡</sup>

Leiden Institute of Chemistry, Gorlaeus Laboratories, Leiden University, PO Box 9502, 2300 RA Leiden, The Netherlands, Shell Research and Technology Center Amsterdam, Shell International Chemicals B.V., PO Box 38000, 1030 BN Amsterdam, The Netherlands, and Department of Crystal and Structural Chemistry, Bijvoet Center for Biomolecular Research, Utrecht University, Utrecht, The Netherlands

Received June 27, 2000

The synthesis of a number of nickel(II) complexes containing the didentate phosphane ligand 1,2-bis(di(*o*-methoxyphenyl)phosphino)ethane (*o*-MeO-dppe) is reported. Two types of complexes have been synthesized, i.e., the mono(chelate) complex (**1**) of the general formula  $[\text{Ni}(o\text{-MeO-dppe})\text{X}_2]$  (where X = Cl, Br or I) and the bis(chelate) complex (**2**) of the general formula  $[\text{Ni}(o\text{-MeO-dppe})_2]\text{Y}_2$  (where Y = PF<sub>6</sub> or trifluoroacetate (TFA)). These complexes have been characterized using electronic absorption and NMR spectroscopy. The structures of the mono(chelate) complex  $[\text{Ni}(o\text{-MeO-dppe})\text{I}_2]$  (**1c**) and of the bis(chelate) complex  $[\text{Ni}(o\text{-MeO-dppe})_2](\text{PF}_6)_2$  (**2e**) have been determined by X-ray crystallography.  $[\text{Ni}(o\text{-MeO-dppe})\text{I}_2]$  crystallizes in the monoclinic space group *P*2<sub>1</sub>/*c* with *Z* = 4, *a* = 12.1309(1) Å, *b* = 16.5759(3) Å, *c* = 17.6474(2) Å, β = 119.3250(10)°.  $[\text{Ni}(o\text{-MeO-dppe})_2](\text{PF}_6)_2$  crystallizes in the monoclinic space group *C*2/*c* with *Z* = 4, *a* = 22.5326(3) Å, *b* = 13.6794(2) Å, *c* = 21.7134(3) Å, β = 107.1745(7)°. In both structures the nickel ion is in a square-planar geometry with a NiP<sub>2</sub>I<sub>2</sub> and NiP<sub>4</sub> chromophore, respectively. Using <sup>1</sup>H and <sup>31</sup>P{<sup>1</sup>H} NMR spectroscopy the behavior of the complexes in various solvents has been studied. It appears that in solution these nickel complexes are involved in an autoionization equilibrium:  $2[\text{Ni}(o\text{-MeO-dppe})\text{X}_2] \rightleftharpoons [\text{Ni}(o\text{-MeO-dppe})_2]^{2+} + [“\text{NiX}_4”]^{2-}$ . The ionized complex (**3**) consists of a cationic unit in which a nickel atom is surrounded by two didentate phosphane ligands, and an anionic unit that stoichiometrically consists of a nickel atom and four anions. The position of the autoionization equilibrium is highly dependent on the anion and the solvent used. In a polar solvent in combination with weakly coordinating anions only the ionized complex is observed, whereas in an apolar solvent in combination with coordinating anions only the mono(chelate) complex occurs. A comparison of the behavior of *o*-MeO-dppe with its unsubstituted analogue dppe in combination with nickel(II) acetate using <sup>31</sup>P{<sup>1</sup>H} NMR spectroscopy shows that the latter is more readily oxidized.

## Introduction

Although nickel is widely used as a heterogeneous catalyst for hydrogenation reactions (Raney nickel), homogeneous hydrogenation catalysts containing nickel are scarcely found in the literature.<sup>1–6</sup> In fact, it is disputable whether the reported nickel complexes yield really homogeneous hydrogenation catalysts or that catalytic hydrogenation activity is due to formation of colloidal (heterogeneous) nickel particles. Yet, homogeneous nickel catalysts are known for related reactions like isomerization, oligomerization, polymerization, hydro-

silylation, and hydrocyanation.<sup>7</sup> Recently, we reported that selected nickel(II) diphosphane complexes are able to hydrogenate homogeneously 1-octene to *n*-octane.<sup>8</sup> Nickel(II) complexes of the *o*-methoxy-substituted didentate phosphane ligands<sup>9</sup> 1,2-bis(di(*o*-methoxyphenyl)phosphino)ethane (*o*-MeO-dppe) or 1,3-bis(di(*o*-methoxyphenyl)phosphino)propane (*o*-MeO-dppp) (see Scheme 1) show catalytic hydrogenation activity in contrast to nickel(II) complexes containing the nonsubstituted didentate phosphane ligands 1,2-bis(diphenylphosphino)ethane (dppe) or 1,3-bis(diphenylphosphino)propane (dppp), which do not show any catalytic hydrogenation activity at all.<sup>8</sup> The origin of the effect of the *o*-methoxy group in the diphosphane ligands *o*-MeO-dppe and *o*-MeO-dppp compared to dppe and dppp on the hydrogenation activity could be steric and/or electronic. The

\* To whom correspondence should be addressed. E-mail: bouwman@chem.leidenuniv.nl and pim.w.p.mul@opc.shell.com.

<sup>†</sup> Leiden University.

<sup>‡</sup> Utrecht University.

<sup>§</sup> Shell International Chemicals B.V.

(1) Emken, E. A.; Frankel, E. N.; Butterfield, R. O. *J. Am. Oil Chem. Soc.* **1966**, *43*, 14.

(2) Itatani, H.; Bailar, J. C., Jr. *J. Am. Chem. Soc.* **1967**, *89*, 1600.

(3) Abley, P.; McQuillin, F. J. *Discuss. Faraday Soc.* **1968**, *46*, 31.

(4) Henrici-Olivé, G.; Olivé, S. *J. Mol. Catal.* **1975/76**, *1*, 121.

(5) Thangaraj, T.; Vancheesan, S.; Rajaram, J.; Kuriacose, J. C. *Indian J. Chem., Sect. A* **1980**, *19*, 404.

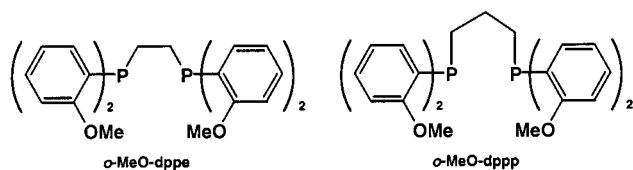
(6) Chatterjee, D.; Bajaj, H. C.; Halligudi, S. B.; Bhatt, K. N. *J. Mol. Catal.* **1993**, *84*, L1.

(7) *Applied Homogeneous Catalysis with Organometallic Compounds*; Cornils, B., Herrmann, W. A., Eds.; VCH Publishers: New York, 1996; Sections 2.3, 2.4, 2.5, and 3.2.14.

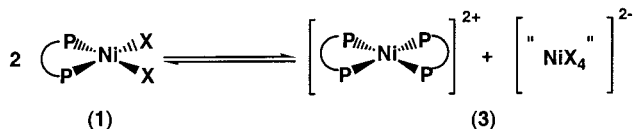
(8) Angulo, I. M.; Kluwer, A. M.; Bouwman, E. *Chem. Commun.* **1998**, 2689.

(9) Abbreviations: TFA = trifluoroacetate, dppe = 1,2-bis(diphenylphosphino)ethane, dppp = 1,3-bis(diphenylphosphino)propane, *o*-MeO-dppe = 1,2-bis(di(*o*-methoxyphenyl)phosphino)ethane, *o*-MeO-dppp = 1,3-bis(di(*o*-methoxyphenyl)phosphino)propane, *p*-MeO-dppp = 1,3-bis(di(*p*-methoxyphenyl)phosphino)propane.

## Scheme 1



## Scheme 2



fact that nickel acetate in combination with a para analogue of the methoxy-substituted ligands (*p*-MeO-dppp) does not show any catalytic hydrogenation activity<sup>8</sup> indicates that the positive effect of the *o*-methoxy groups on the hydrogenation activity is predominantly steric.

A hypothesis to explain the difference in catalytic activity of nickel complexes containing *o*-MeO-dppe versus dppe concerns the autoionization equilibrium depicted in Scheme 2. Two mono(chelate) complexes (1) react to form an ionized complex (3), which consists of a bis(chelate) cationic unit and an anionic unit formally containing one nickel atom and four anions. This autoionization reaction was already observed by Jarrett et al.,<sup>10</sup> while studying the solid-state and solution chemistry of Ni(II) complexes containing the ligand dppe. It is assumed that the resulting ionized complex (3) is unable to act as a catalyst in the hydrogenation of 1-octene. This assumed catalytic inactivity is rationalized by the lack of available sites for coordination of the reactants in the cationic unit, whereas the anionic unit in 3, containing "naked" nickel (i.e., not containing a didentate phosphane ligand), is only expected to yield an active catalyst at higher temperatures, when colloidal nickel particles are formed.<sup>11</sup>

It was surmised that the *o*-methoxy groups could prevent the formation of the inactive ionized complex due to their bulkiness, hampering the complexation of a second didentate phosphane ligand to the nickel ion. Therefore, a study was undertaken to investigate the nature of species in solution for both *o*-methoxy-containing ligands *o*-MeO-dppe and *o*-MeO-dppp. This manuscript describes the results of the NMR investigation on the autoionization equilibrium of nickel complexes containing the didentate phosphane ligand *o*-MeO-dppe. The results of the complementary investigation concerning *o*-MeO-dppp as the ligand will be reported elsewhere,<sup>12</sup> as it showed quite different behavior which is not directly related with that described in this manuscript.

## Experimental Section

**General Procedures.** Melting points were determined on a Büchi apparatus and are uncorrected. Elemental analyses were performed on a Perkin-Elmer 2400 series II analyzer. Mass spectra were obtained with a Finnigan MAT TSQ-700 mass spectrometer equipped with a custom-made electrospray interface (ESI). Spectra were collected by constant infusion of the analyte dissolved in methanol/water with 1% HOAc. Nickel complexes were analyzed by electrospray mass spectrometry using a Micromass Quattro triple-quadrupole mass spectrometer. Mass spectra were collected both in positive and in negative mode,

showing cationic and anionic complex fragments, respectively. Samples of nickel complexes were dissolved in methanol and introduced by infusion in a methanol flow. Infrared spectra were recorded with a Perkin-Elmer Paragon 1000 IR spectrophotometer equipped with a Golden Gate ATR device, using the reflectance technique (4000–300 cm<sup>-1</sup>). Solid-state electronic absorption spectra were obtained on a Perkin-Elmer Lambda 900 spectrophotometer using the diffuse reflectance technique, with MgO as a reference. The electronic absorption spectra in solution were taken using 1 cm path length cells at ambient temperature, with the used solvent as the reference. The <sup>1</sup>H NMR and <sup>31</sup>P{<sup>1</sup>H} NMR spectra were recorded on a Varian VXR-200 spectrometer at 200.06 and 80.98 MHz, respectively, or on a Bruker WM-300 spectrometer at 300.13 and 121.50 MHz, respectively. The high-pressure NMR experiments were conducted on a Varian INOVA-400 spectrometer operating at 399.97 MHz for <sup>1</sup>H NMR and at 161.91 MHz for <sup>31</sup>P{<sup>1</sup>H} NMR. The <sup>31</sup>P and <sup>1</sup>H chemical shifts were recorded in δ units relative to triphenylphosphane (–6 ppm) and the deuterated solvent (CD<sub>2</sub>Cl<sub>2</sub>, 5.24 ppm; CD<sub>3</sub>OD, 3.35 ppm), respectively. The <sup>1</sup>H NMR and <sup>31</sup>P{<sup>1</sup>H} NMR data of the ligand and the nickel complexes in CD<sub>2</sub>Cl<sub>2</sub> are collected in Table 1.

**Syntheses.** All chemicals were reagent grade and were used as received or synthesized as described below. Reactions were carried out under an atmosphere of dry argon or dry nitrogen, unless stated otherwise, using standard Schlenk techniques. Tris(*o*-methoxyphenyl)phosphane was synthesized according to a literature procedure.<sup>13</sup> Generally the complexes were obtained in yields of 30–50%; no attempts have been undertaken to optimize the yields.

**1,2-Bis(di(*o*-methoxyphenyl)phosphino)ethane (*o*-MeO-dppe).** This synthesis was performed according to the procedure earlier described for the synthesis of 1,3-bis(di(*o*-methoxyphenyl)phosphino)propane.<sup>14</sup> The synthesis was performed under an argon atmosphere. It is important that absolutely no air or water is present during the reaction. A 250 mL round-bottom flask was equipped with an argon inlet, a condenser, an ammonia inlet, and a magnetic stirrer bar. While the flask was cooled with an acetone/dry ice mixture, 100 mL of dry ammonia was condensed into the flask. Traces of water were removed from the ammonia by addition of a small piece of sodium metal (10 mg). To the liquid ammonia was added 60 mmol (1.4 g) of sodium metal through the condenser. After 15 min 30 mmol (10.6 g) of tris(*o*-methoxyphenyl)phosphane was slowly added through the condenser to the blue solution, followed by 25 mL of dry and peroxide-free THF. The blue mixture turned deep orange/red within 1 h of stirring. After 5 h of stirring, while the temperature was kept between –78 and –50 °C, 30 mmol (1.6 g) of anhydrous ammonium chloride was added. After 15 min 15 mmol (1.5 g) of 1,2-dichloroethane in 15 mL of THF was added. The temperature was allowed to rise to room temperature, and the ammonia was allowed to evaporate overnight. The remaining part of the synthesis of the ligand could be performed in air. The solvent was removed in vacuo, and the residue was dissolved in dichloromethane, to which an aqueous solution of ammonium chloride was then added. The organic layer was separated, dried with sodium sulfate, and filtered. The organic solvent was removed in vacuo. The white/yellow oil was treated with methanol, resulting in a white precipitate. The white solid was collected by filtration and washed with methanol. Drying in vacuo gave 6.3 g (12.2 mmol), 81% yield; mp 180–4 °C. Anal. Calcd for C<sub>30</sub>H<sub>32</sub>O<sub>4</sub>P<sub>2</sub> (fw = 518.5): C, 69.49; H, 6.22. Found: C, 68.15; H, 6.15. MS (ESI): *m/z* 519 [M + H]<sup>+</sup>.

**[Ni(*o*-MeO-dppe)Cl<sub>2</sub>] (1a). Method A.** Ni(OAc)<sub>2</sub>·4H<sub>2</sub>O (50 mg, 0.20 mmol) was mixed with an equimolar amount of *o*-MeO-dppe (104 mg, 0.20 mmol) in 20 mL of ethanol. The mixture was refluxed for 3½ hours, and a clear orange solution was obtained. After the solution was partly cooled, 0.5 mL of hydrochloric acid was added (1 M in Et<sub>2</sub>O, 0.5 mmol). After several minutes an orange precipitate had formed. The solid was collected by filtration and dried in air.

**Method B.** NiCl<sub>2</sub>·6H<sub>2</sub>O (370 mg, 1.57 mmol) was dissolved in 10 mL of ethanol and mixed with *o*-MeO-dppe (520 mg, 1.00 mmol) dissolved in 10 mL of chloroform. Immediately a dark orange solution

(10) Jarrett, P. S.; Sadler, P. J. *Inorg. Chem.* **1991**, *30*, 2098.

(11) Kelber, C. *Ber. Dtsch. Chem. Ges.* **1917**, *50*, 1509.

(12) Angulo, I. M.; Bouwman, E.; Lok, S. M.; Lutz, M.; Mul, W. P.; Spek, A. L. *Eur. J. Inorg. Chem.*, in press.

(13) Brandsma, L.; Verkruisje, H. D. *Synth. Comm.* **1990**, *20*, 2273.

(14) Budzelaar, P. H. M.; van Doorn, J. A.; Meijboom, N. *Recl. Trav. Chim. Pays-Bas* **1991**, *110*, 420.

**Table 1.**  $^1\text{H}$  NMR and  $^{31}\text{P}\{^1\text{H}\}$  NMR Data of *o*-MeO-dppe and Nickel Complexes in  $\text{CD}_2\text{Cl}_2$  at 25 °C

	$^1\text{H}$ NMR			$^{31}\text{P}\{^1\text{H}\}$ NMR
	–C <sub>6</sub> H <sub>4</sub>	–OCH <sub>3</sub>	–CH <sub>2</sub> CH <sub>2</sub> –	
<i>o</i> -MeO-dppe	6.78 (t, 8H), 6.95 (m, 4H), 7.22 (t, 4H)	3.64 (s, 12H)	2.01 (t, 4H)	–31.67
[Ni( <i>o</i> -MeO-dppe)Cl <sub>2</sub> ] ( <b>1a</b> )	6.90 (d, 4H), 6.96 (t, 4H), 7.48 (t, 4H), 8.13 (m, 4H)	3.56 (s, 12H)	2.39 (d, 4H)	58.24
[Ni( <i>o</i> -MeO-dppe)Br <sub>2</sub> ] ( <b>1b</b> )	6.88 (d, 4H), 6.98 (t, 4H), 7.46 (t, 4H), 8.13 (m, 4H)	3.56 (s, 12H)	2.35 (d, 4H)	66.03
[Ni( <i>o</i> -MeO-dppe)I <sub>2</sub> ] ( <b>1c</b> )	6.88 (d, 4H), 6.97 (t, 4H), 7.43 (t, 4H), 8.06 (m, 4H)	3.57 (s, 12H)	2.39 (d, 4H)	75.63
[Ni( <i>o</i> -MeO-dppe) <sub>2</sub> ](TFA) <sub>2</sub> ( <b>2d</b> )	5.77 (m, 2H), 6.49 (t, 2H), 6.69 (d, 2H), 6.93 (d, 2H), 7.23 (m, 4H), 7.72 (t, 2H), 8.58 (m, 2H)	3.42 (s, 6H), 3.47 (s, 6H)	2.23 (d, 2H), 2.83 (m, 2H)	52.70
[Ni( <i>o</i> -MeO-dppe) <sub>2</sub> ](PF <sub>6</sub> ) <sub>2</sub> ( <b>2e</b> )	5.75 (m, 2H), 6.48 (t, 2H), 6.67 (d, 2H), 6.91 (d, 2H), 7.21 (m, 4H), 7.70 (t, 2H), 8.59 (m, 2H)	3.41 (s, 6H), 3.46 (s, 6H)	2.23 (d, 2H), 2.83 (m, 2H)	54.40, –143.9 (septet, PF <sub>6</sub> )
[Ni( <i>o</i> -MeO-dppe)(TFA) <sub>2</sub> ] ( <b>1d</b> ) or [Ni( <i>o</i> -MeO-dppe) <sub>2</sub> ][Ni(TFA) <sub>4</sub> ] ( <b>3d</b> )	<i>a</i>			52.70, 53.76

<sup>a</sup> In  $\text{CD}_2\text{Cl}_2$  a mixture of **1d** and **3d** is observed, see Table 4 and discussion.

was obtained, and an orange solid precipitated within a few minutes. The solid was collected by filtration and dried in air.

Anal. Calcd for  $\text{C}_{30}\text{H}_{32}\text{Cl}_2\text{NiO}_4\text{P}_2$  (fw = 648.13): C, 55.60; H, 4.98. Found: C, 54.95; H, 4.55. Diffuse reflectance electronic absorption of the solid:  $\nu_{\text{max}}$  28 100 and 21 200  $\text{cm}^{-1}$ . Electronic absorption in  $\text{CH}_2\text{Cl}_2$  (molar extinction coefficients ( $\text{L mol}^{-1} \text{cm}^{-1}$ )):  $\nu_{\text{max}}$  31 900  $\text{cm}^{-1}$  (19 700) and 21 300  $\text{cm}^{-1}$  (1200).

[Ni(*o*-MeO-dppe)Br<sub>2</sub>] (**1b**). NiBr<sub>2</sub> (220 mg, 1.00 mmol) was dissolved in 10 mL of ethanol, and *o*-MeO-dppe (520 mg, 1.00 mmol) was dissolved in 10 mL of chloroform. The solution containing NiBr<sub>2</sub> was filtered before it was added to the ligand solution. When both solutions were mixed, a dark red solution was obtained. After several minutes a dark red solid precipitated from the solution. The solid was collected by filtration and dried in air. Anal. Calcd for  $\text{C}_{30}\text{H}_{32}\text{Br}_2\text{NiO}_4\text{P}_2$  (fw = 737.03): C, 48.89; H, 4.38. Found: C, 49.66; H, 4.48. Diffuse reflectance electronic absorption of the solid:  $\nu_{\text{max}}$  30 100 and 20 900  $\text{cm}^{-1}$ .

[Ni(*o*-MeO-dppe)I<sub>2</sub>] (**1c**). Ni(OAc)<sub>2</sub>·4H<sub>2</sub>O (83 mg, 0.33 mmol) was dissolved in 10 mL of ethanol, and *o*-MeO-dppe (172 mg, 0.33 mmol) was dissolved in 10 mL of chloroform. When both solutions were mixed, an orange solution was obtained. Then 0.08 mL of concentrated hydrogen iodide (50% in water, 0.64 mmol) was added and a purple solution was obtained. After some days purple crystals precipitated from the solution. These crystals were suitable for X-ray diffraction. Anal. Calcd for  $\text{C}_{30}\text{H}_{32}\text{I}_2\text{NiO}_4\text{P}_2$  (fw = 831.03): C, 43.36; H, 3.88. Found: C, 43.17; H, 3.53. Diffuse reflectance electronic absorption of the solid:  $\nu_{\text{max}}$  28 200 and 19 200  $\text{cm}^{-1}$ .

[Ni(*o*-MeO-dppe)<sub>2</sub>](TFA)<sub>2</sub> (**2d**). Ni(OAc)<sub>2</sub>·4H<sub>2</sub>O (130 mg, 0.52 mmol) was mixed with *o*-MeO-dppe (530 mg, 1.02 mmol) in a mixture of 10 mL of dichloromethane and 1 mL of methanol. When a clear orange solution was obtained, 0.1 mL of trifluoroacetic acid was added (1.3 mmol). The solvent was partly evaporated and diethyl ether was added, resulting in a yellow precipitate. The solvent was decanted, and the solid was dried in air. Anal. Calcd for  $\text{C}_{64}\text{H}_{64}\text{F}_6\text{NiO}_{12}\text{P}_4\cdot\text{CH}_2\text{Cl}_2$  (fw = 1406.71): C, 55.50; H, 4.73. Found: C, 55.01; H, 4.59. Diffuse reflectance electronic absorption of the solid:  $\nu_{\text{max}}$  28 900  $\text{cm}^{-1}$ .

[Ni(*o*-MeO-dppe)<sub>2</sub>](PF<sub>6</sub>)<sub>2</sub> (**2e**). Ni(OAc)<sub>2</sub>·4H<sub>2</sub>O (125 mg, 0.50 mmol) was dissolved in 15 mL of ethanol, and *o*-MeO-dppe (570 mg, 1.10 mmol) was dissolved in 15 mL of chloroform. When both solutions were mixed, a red solution was obtained. Then NH<sub>4</sub>PF<sub>6</sub> (160 mg, 0.98 mmol) dissolved in 5 mL of ethanol was added and an orange solution was obtained. After several days an orange solid precipitated from the solution. Recrystallization from a methanol/dichloromethane mixture yielded crystals which were suitable for X-ray diffraction. Anal. Calcd for  $\text{C}_{60}\text{H}_{64}\text{F}_{12}\text{NiO}_8\text{P}_6\cdot(\text{CHCl}_3)_2$  (fw = 1624.43): C, 45.84; H, 4.10. Found: C, 46.05; H, 3.90. Diffuse reflectance electronic absorption of the solid:  $\nu_{\text{max}}$  28 000  $\text{cm}^{-1}$ . Electronic absorption in  $\text{CH}_2\text{Cl}_2$  (molar

extinction coefficients ( $\text{L mol}^{-1} \text{cm}^{-1}$ ):  $\nu_{\text{max}}$  34 000  $\text{cm}^{-1}$  (34 200), 29 600  $\text{cm}^{-1}$  (16 000), and 28 000  $\text{cm}^{-1}$  (shoulder).

[Ni(*o*-MeO-dppe)(TFA)<sub>2</sub>] (**1d**) or [Ni(*o*-MeO-dppe)<sub>2</sub>][Ni(TFA)<sub>4</sub>] (**3d**). Ni(OAc)<sub>2</sub>·4H<sub>2</sub>O (72 mg, 0.29 mmol) and an equimolar amount of *o*-MeO-dppe (150 mg, 0.29 mmol) were mixed in 50 mL ethanol. This mixture was brought to reflux temperature, and after 16 h the bright orange solution was cooled. After the mixture was concentrated to approximately 5 mL under vacuum, 45 mL of toluene was added and the mixture brought to reflux temperature for 15 min to afford an orange/red solution. When the reaction mixture was cooled to 40 °C, 0.07 mL of trifluoroacetic acid was added (0.92 mmol). After removal of half of the solvent under vacuum, an orange precipitate was formed overnight, which was isolated by filtration and washed twice with hexane. Anal. Calcd for  $\text{C}_{34}\text{H}_{32}\text{F}_6\text{NiO}_8\text{P}_2$  (**1d**) (fw = 803.25) or  $\text{C}_{68}\text{H}_{64}\text{F}_{12}\text{Ni}_2\text{O}_{16}\text{P}_4$  (**3d**) (fw = 1606.49): C, 50.84; H, 4.02. Found: C, 48.52; H, 3.80. Diffuse reflectance electronic absorption of the solid: three weak signals were observed at  $\nu$  8500, 13 500, and 20 800  $\text{cm}^{-1}$  (shoulder). Following this procedure, it is inevitable that some physical mixture may be obtained or some impurities are present, explaining the rather poor elemental analysis. The compound, however, is essential for the NMR experiments described in this manuscript.

**X-ray Crystal Structure Determinations of [Ni(*o*-MeO-dppe)I<sub>2</sub>] (**1c**) and [Ni(*o*-MeO-dppe)<sub>2</sub>](PF<sub>6</sub>)<sub>2</sub> (**2e**).** Intensities were measured on a Nonius KappaCCD diffractometer with rotating anode (Mo K $\alpha$ ,  $\lambda$  = 0.710 73 Å) at 150 K. The structures were solved with Patterson methods (DIRDIF-97<sup>15</sup>) and refined with the program SHELXL-97<sup>16</sup> against  $F^2$  of all reflections up to a resolution of  $(\sin \theta/\lambda)_{\text{max}}$  = 0.65 Å<sup>-1</sup>. Non-hydrogen atoms were refined freely with anisotropic displacement parameters, and hydrogen atoms were refined as rigid groups. The drawings, structure calculations, and checking for higher symmetry were performed with the program PLATON.<sup>17</sup> Further experimental details are given in Table 2.

The crystal structure of **2e** contains large voids (520 Å<sup>3</sup>) filled with disordered solvent molecules (methanol and dichloromethane). Their contribution to the structure factors was secured by back-Fourier transformation (program PLATON,<sup>17</sup> CALC SQUEEZE, 123 e<sup>-</sup>/unit cell).

**NMR Studies.** Both  $^1\text{H}$  NMR and  $^{31}\text{P}\{^1\text{H}\}$  NMR spectra of the above-mentioned complexes were taken in the solvents methanol-*d*<sub>4</sub>,

- Beurskens, P. T.; Admiraal, G.; Beurskens, G.; Bosman, W. P.; Garcia-Granda, S.; Gould, R. O.; Smits, J. M. M.; Smykalla, C. The DIRDIF97 program system. Technical Report of the Crystallography Laboratory; University of Nijmegen: Nijmegen, The Netherlands; 1997.
- Sheldrick, G. M. *SHELXL97. Program for crystal structure refinement*; University of Göttingen: Göttingen, Germany, 1997.
- Spek, A. L. *PLATON. A multipurpose crystallographic tool*; Utrecht University: Utrecht, The Netherlands, 2000.



**Table 2.** Crystal Data and Structure Refinement Details for [Ni(*o*-MeO-dppe)<sub>2</sub>]<sub>2</sub> (**1c**) and [Ni(*o*-MeO-dppe)<sub>2</sub>](PF<sub>6</sub>)<sub>2</sub> (**2e**)

	<b>1c</b>	<b>2e</b>
formula	C <sub>30</sub> H <sub>32</sub> I <sub>2</sub> NiO <sub>4</sub> P <sub>2</sub>	C <sub>60</sub> H <sub>64</sub> NiO <sub>8</sub> P <sub>4</sub> ·2PF <sub>6</sub> + solvent
fw	831.01	1385.64 <sup>a</sup>
space group	<i>P</i> <sub>2</sub> / <i>c</i> (No. 14)	<i>C</i> 2/ <i>c</i> (No. 15)
<i>a</i> (Å)	12.1309(1)	22.5326(3)
<i>b</i> (Å)	16.5759(3)	13.6794(2)
<i>c</i> (Å)	17.6474(2)	21.7134(3)
$\beta$ (deg)	119.3250(10)	107.1745(7)
<i>V</i> (Å <sup>3</sup> )	3093.82(7)	6394.34(15)
<i>Z</i>	4	4
$\rho_{\text{calc}}$ (g cm <sup>-3</sup> )	1.784	1.439 <sup>a</sup>
$\mu$ (mm <sup>-1</sup> )	2.76	0.54 <sup>a</sup>
R1 <sup>b</sup> (obs/all reflns)	0.0278/0.0362	0.0340/0.0400
wR2 <sup>c</sup> (obs/all reflns)	0.0672/0.0703	0.0935/0.0974

<sup>a</sup> Derived values do not contain the contribution of the disordered solvent molecules. <sup>b</sup>  $R1 = \sum |F_o| - |F_c| / \sum |F_o|$ . <sup>c</sup>  $wR2 = [\sum w(F_o^2 - F_c^2)^2 / \sum w(F_o^2)]^{1/2}$ ,  $w = 1/[\sigma^2(F_o^2) + (AP)^2 + BP]$  where  $P = (F_o^2 + 2F_c^2)/3$ ,  $A = 0.0355$  (**1c**) or 0.0530 (**2e**), and  $B = 2.6536$  (**1c**) or 4.8452 (**2e**).

dichloromethane-*d*<sub>2</sub>, acetone-*d*<sub>6</sub>, and toluene-*d*<sub>8</sub>. All deuterated solvents were reagent grade and were used as received. For the high-pressure NMR experiments, the sapphire NMR tube was pressurized with 10 bar of dihydrogen gas.

For the in situ experiments Ni(OAc)<sub>2</sub>·4H<sub>2</sub>O (5.0 mg, 0.02 mmol) and the ligand, *o*-MeO-dppe (9.1 mg, 0.02 mmol) or dppe (7.0 mg, 0.02 mmol), were mixed in the NMR tube. The nickel salt and the ligand were weighed into an NMR tube, which was then evacuated and filled with nitrogen three successive times. Under a nitrogen stream the deuterated solvent was added. The solution was analyzed when, sometimes after filtration, a clear solution was obtained.

For the analysis of a spent catalyst, a hydrogenation experiment was carried out. Ni(OAc)<sub>2</sub>·4H<sub>2</sub>O (25 mg, 0.1 mmol) and *o*-MeO-dppe (57 mg, 0.11 mmol), *o*-MeO-dppp (59 mg, 0.11 mmol), or dppp (45 mg, 0.11 mmol) were mixed in 10 mL of methanol and 10 mL of dichloromethane. To the clear solution was added 7.5 mL of 1-octene (50 mmol), and the solution was loaded into the autoclave. The hydrogenation experiment was performed at 50 bar of hydrogen pressure and 50 °C. After 30 min, the solution was extracted from the autoclave into a round-bottom flask under an inert atmosphere. The solvent was evaporated, and the resulting solid was dissolved in deuterated methanol for NMR analysis.

## Results and Discussion

**Syntheses.** The ligand *o*-MeO-dppe was prepared using the method based on the earlier reported reductive splitting of tris(*o*-methoxyphenyl)phosphane (P(*o*-MeO-Ph)<sub>3</sub>) using sodium in ammonia.<sup>14</sup> It is important that absolutely no water is present during this reductive splitting. Even traces of water lead to an incomplete splitting of P(*o*-MeO-Ph)<sub>3</sub> and contamination of the resulting product with starting material P(*o*-MeO-Ph)<sub>3</sub>, which cannot be removed. The <sup>31</sup>P{<sup>1</sup>H} NMR spectrum of the ligand in CD<sub>2</sub>Cl<sub>2</sub> shows a singlet at -31.7 ppm. The bridging ethylene protons appear as a virtual triplet, due to coupling with the two phosphorus atoms, at 2.0 ppm in the <sup>1</sup>H NMR spectrum, which further shows a singlet at 3.64 ppm, corresponding to the protons of the *o*-methoxy groups. With the obtained ligand a number of nickel(II) complexes were synthesized varying the anions and with various ligand-to-metal ratios. Although it is known that in general phosphane ligands are sensitive toward oxidation, the obtained complexes appeared to be stable in air. An overview of the synthesized compounds is given in Scheme 3. With halide anions, mono(*o*-MeO-dppe) complexes of the type [Ni(*o*-MeO-dppe)X<sub>2</sub>] (X = Cl (**1a**), Br (**1b**), or I (**1c**)) were

## Scheme 3

<b>mono(ligand) complex</b>	<b>1a</b> [Ni( <i>o</i> -MeO-dppe)Cl <sub>2</sub> ] <b>1b</b> [Ni( <i>o</i> -MeO-dppe)Br <sub>2</sub> ] <b>1c</b> [Ni( <i>o</i> -MeO-dppe)I <sub>2</sub> ] <b>1d</b> [Ni( <i>o</i> -MeO-dppe)(TFA) <sub>2</sub> ]
<b>bis(ligand) complex</b>	<b>2d</b> [Ni( <i>o</i> -MeO-dppe) <sub>2</sub> ](TFA) <sub>2</sub> <b>2e</b> [Ni( <i>o</i> -MeO-dppe) <sub>2</sub> ](PF <sub>6</sub> ) <sub>2</sub>
<b>ionized complex</b>	<b>3d</b> [Ni( <i>o</i> -MeO-dppe) <sub>2</sub> ][Ni(TFA) <sub>4</sub> ]

synthesized. Using a ligand-to-metal ratio of two and more weakly coordinating anions, bis(*o*-MeO-dppe) complexes of the type [Ni(*o*-MeO-dppe)<sub>2</sub>]Y<sub>2</sub> (Y = trifluoroacetate (TFA) (**2d**) or PF<sub>6</sub> (**2e**)) were obtained. Finally, an attempt was undertaken to synthesize the mono(chelate) complex [Ni(*o*-MeO-dppe)-(TFA)<sub>2</sub>] (**1d**). As this complex contains the weakly coordinating anion TFA, the formulation of this compound could also be given as [Ni(*o*-MeO-dppe)<sub>2</sub>][Ni(TFA)<sub>4</sub>] (**3d**), being the ionized complex (see below). In order to synthesize this complex, nickel(II) acetate and *o*-MeO-dppe were mixed in a 1:1 ratio in the polar solvent ethanol, leading to the ionized complex [Ni(*o*-MeO-dppe)<sub>2</sub>][Ni(OAc)<sub>4</sub>]. With the aim to form complex **1d** most of the ethanol was evaporated and replaced by the apolar solvent toluene, before trifluoroacetic acid was added to replace the acetate anions.

**Characterization of the Synthesized Complexes in the Solid Phase.** The infrared spectra of all synthesized nickel(II) complexes are very similar to each other and also to that of the free ligand *o*-MeO-dppe. Unfortunately, because of the lack of differences, infrared spectroscopy cannot be used to distinguish a mono(chelate) complex (**1**) from a bis(chelate) complex (**2**). The diffuse reflectance absorption spectra of both types of complexes proved more useful, as these show some clear differences. In the absorption spectrum of a mono(chelate) complex [Ni(*o*-MeO-dppe)X<sub>2</sub>] (**1**) only one band at around 20 000 cm<sup>-1</sup> is observed. Strong bands at higher energies are attributed to charge-transfer transitions. The band around 20 000 cm<sup>-1</sup>, which is ascribed to the <sup>1</sup>A<sub>1</sub> → <sup>1</sup>B<sub>2</sub> transition, is typical for a square-planar nickel complex containing one didentate phosphane ligand.<sup>18</sup> In the absorption spectrum of a bis(chelate) complex [Ni(*o*-MeO-dppe)<sub>2</sub>]Y<sub>2</sub> (**2**) only charge-transfer bands are observed. It is known that the bands characteristic of the NiP<sub>4</sub> chromophore should lie at higher energies than those for the NiP<sub>2</sub>X<sub>2</sub> chromophore.<sup>19</sup> The bands due to NiP<sub>4</sub> apparently fall in the region obscured by strong charge-transfer absorptions. As no other bands are observed in the absorption spectra of these bis(chelate) complexes, they are tentatively ascribed square-planar geometry.

In an attempt to synthesize the mono(chelate) complex [Ni(*o*-MeO-dppe)(TFA)<sub>2</sub>] (**1d**), an orange complex was obtained, for which elemental analysis showed the metal-to-ligand ratio to be 1. Although this ratio is as expected for the desired mono(chelate) complex **1d**, it also corresponds to the ionized complex **3d**. In the diffuse reflectance absorption spectrum of the obtained orange solid only three weak bands, tentatively assigned to an octahedral complex,<sup>19</sup> are observed, apart from the strong charge-transfer bands. For **1d** the band corresponding to the mono(chelate) complex with an NiP<sub>2</sub>O<sub>2</sub> chromophore is expected to lie at a higher energy than that of [Ni(*o*-MeO-dppe)-Cl<sub>2</sub>], according to the established spectrochemical series.<sup>19</sup> It is even possible that this band will disappear under the charge-

(18) van Hecke, G. R.; Horrocks, W. DeW., Jr. *Inorg. Chem.* **1966**, *5*, 1968.

(19) Lever, A. B. P. *Inorganic Electronic Spectroscopy*; Elsevier: Amsterdam, 1983; Section 6.2.

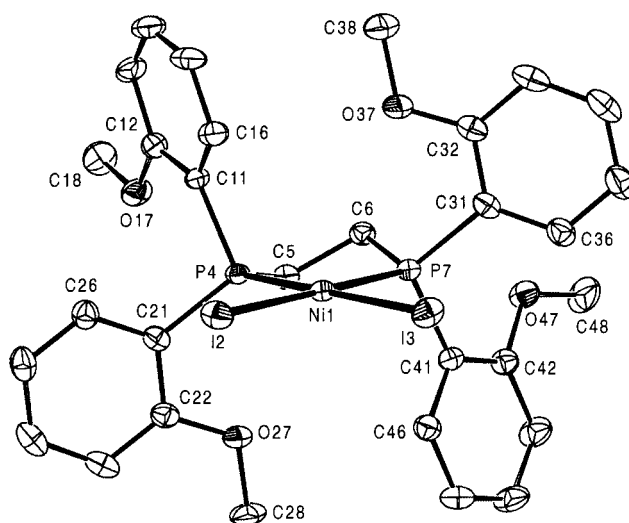
**Table 3.** Selected Interatomic Distances, Angles, and Torsion Angles for [Ni(*o*-MeO-dppe)I<sub>2</sub>] (**1c**) and [Ni(*o*-MeO-dppe)<sub>2</sub>](PF<sub>6</sub>)<sub>2</sub> (**2e**). A Comparison Is Made with the Analogous Complexes with the Unsubstituted Ligand dppe, [Ni(dppe)Cl<sub>2</sub>]·CH<sub>2</sub>Cl<sub>2</sub> (Form B) (**I**)<sup>20,21</sup> and [Ni(dppe)<sub>2</sub>](NO<sub>3</sub>)<sub>2</sub> (**II**)<sup>23 a,b</sup>

[Ni( <i>o</i> -MeO-dppe)I <sub>2</sub> ] ( <b>1c</b> ) X = I		[Ni(dppe)Cl <sub>2</sub> ] ( <b>I</b> ) (form B) X = Cl	Ni( <i>o</i> -MeO-dppe) <sub>2</sub> (PF <sub>6</sub> ) <sub>2</sub> ( <b>2e</b> )		[Ni(dppe) <sub>2</sub> ](NO <sub>3</sub> ) <sub>2</sub> ( <b>II</b> )
Distances (Å)					
Ni1–X2	2.5442(4)	2.195(2)			
Ni1–X3	2.5214(5)	2.205(2)			
Ni1–P4	2.1789(9)	2.157(2)	Ni1–P4	2.2732(5)	2.261(3)
Ni1–P7	2.1776(7)	2.145(2)	Ni1–P7	2.2724(5)	2.256(3)
Ni1–O27	3.773(2)		Ni1–O17	3.9300(14)	
Ni1–O37	3.636(2)	–	Ni1–O47	3.9317(14)	
Ni1–H16	2.7913	2.745	Ni1–H26	2.7299	3.112
Ni1–H46	2.7786	2.770	Ni1–H36	2.6532	2.625
Angles (deg)					
X2–Ni1–X3	92.88(1)	95.47(6)	P7–Ni1–P4	96.61(1)	96.75
X2–Ni1–P4	91.29(2)	89.01(6)			
X2–Ni1–P7	177.77(3)	175.06(7)	P7–Ni1–P4a	179.35(2)	180.00
X3–Ni1–P4	175.56(2)	175.19(6)			
X3–Ni1–P7	89.35(3)	88.68(6)	P7–Ni1–P7a	83.34(2)	83.25(12)
P4–Ni1–P7	86.48(3)	86.93(6)	P4–Ni1–P4a	83.44(2)	83.25(12)
Torsion Angles (deg)					
Ni1–P4–C11–C12	165.5(2)	174.88	Ni1–P4–C11–C12	72.44(14)	68.26
Ni1–P4–C21–C22	–70.9(3)	–85.66	Ni1–P4–C21–C22	–164.72(13)	–166.46
Ni1–P7–C31–C32	–66.0(3)	–78.87	Ni1–P7–C31–C32	–170.96(13)	–174.83
Ni1–P7–C41–C42	176.3(2)	172.91	Ni1–P7–C41–C42	74.66(15)	73.12
P4–C5–C6–P7	48.5(2)	47.85	P4–C5–C5a–P4a	–55.15(13)	30.82(15)
			P7–C6–C6a–P7a	–51.85(14)	30.82(15)

<sup>a</sup> Although the atom numbering and symmetry of the complexes [Ni(dppe)Cl<sub>2</sub>]·CH<sub>2</sub>Cl<sub>2</sub> (form B) (**I**) and [Ni(dppe)<sub>2</sub>](NO<sub>3</sub>)<sub>2</sub> (**II**) are not the same as those in our compounds, the values listed in the table are arranged in such a way that the like atoms are compared. <sup>b</sup> Values for [Ni(dppe)Cl<sub>2</sub>]·CH<sub>2</sub>Cl<sub>2</sub> (form B) (**I**) and [Ni(dppe)<sub>2</sub>](NO<sub>3</sub>)<sub>2</sub> (**II**) which could not be found in the report were calculated, without standard deviations, with the program PLATON<sup>17</sup> using the atomic coordinates as retrieved from CCDC (**I**, FUJXUD; **II**, VASCIB).

transfer bands. Thus, unfortunately, even electronic absorption spectroscopy is not helpful to assign unambiguously either formulation **1d** or **3d** to the isolated compound, as for either of the two compounds also the occurrence of a slight octahedral distortion can be explained. In **1d** this distortion could be caused by a complex in which the TFA anions are coordinated in a didentate fashion to the nickel ion, whereas in **3d** the anionic unit of the ionized complex could be the source of the bands assigned to an octahedral complex.

**Crystal Structure of [Ni(*o*-MeO-dppe)I<sub>2</sub>] (**1c**).** A molecular plot of the structure showing 50% probability ellipsoids is given in Figure 1. Selected interatomic distances and angles are given in Table 3. The present structure of [Ni(*o*-MeO-dppe)I<sub>2</sub>] (**1c**) largely resembles that of the related structure of [Ni(dppe)Cl<sub>2</sub>]·CH<sub>2</sub>Cl<sub>2</sub> (**I**).<sup>20,21</sup> In Table 3 the relevant bond distances and angles are compared, whereas in Figure 2a the two compounds are compared in a graphical representation. The coordination geometry around the nickel(II) center in both complexes is essentially square-planar. In both structures the dihedral angle between the X–Ni–X and P–Ni–P planes does not differ considerably from zero (1.53° in **1c** and 3.30° in **I**). The Ni–P distances in **1c** are slightly longer than those in **I**. The bite angle P–Ni–P is essentially the same in the two compounds. It is possible to distinguish the aryl rings as oriented either axially (rings 1 and 4) or equatorially (rings 2 and 3) with respect to the five-membered chelate ring. This orientation of the aryl rings is essentially the same as in **I**, as can be seen in Figure 2a. The *o*-methoxy groups of the axial aryl rings in **1c** are pointing away from the central nickel atom (torsion angles Ni1–P4–C11–

**Figure 1.** Displacement ellipsoid plot (50% probability) of [Ni(*o*-MeO-dppe)I<sub>2</sub>] (**1c**) with atom-labeling scheme. Hydrogen atoms are omitted for clarity.

C12 = 165.5(2)° and Ni1–P7–C41–C42 = 176.3(2)°, in contrast to the *o*-methoxy groups of the equatorial aryl rings, which are more pointing toward the nickel atom (torsion angles Ni1–P4–C21–C22 = –70.9(3)° and Ni1–P7–C31–C32 = –66.0(3)°). However, the corresponding Ni···O distances of 3.773(2) Å (O27) and 3.636(2) Å (O37) are too large to consider an electrostatic interaction. In Figure 1 it can be seen that the *o*-hydrogen atoms of the axial aryl groups are pointing toward the nickel atom. The Ni···H distances of 2.79 Å (H16) and 2.78 Å (H46) indicate the presence of either agostic interactions or Ni···H–C hydrogen bonds, a phenomenon which has been

(20) Spek, A. L.; van Eijck, B. P.; Jans, R. J. F.; van Koten, G. *Acta Crystallogr.* **1987**, C43, 1878.

(21) Busby, R.; Hursthouse, M. B.; Jarrett, P. S.; Lehmann, C. W.; Malik, K. M. A.; Phillips, C. J. *Chem. Soc., Dalton Trans.* **1993**, 3767.

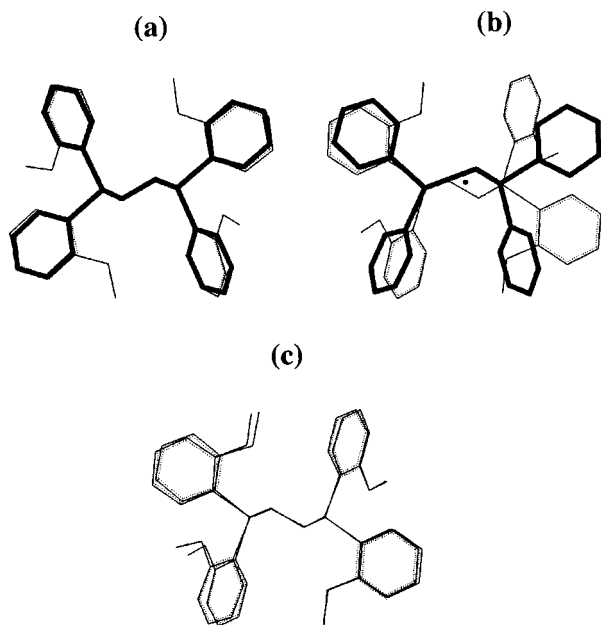


**Figure 2.** (a) Crystal structures of  $[\text{Ni}(o\text{-MeO-dppe})_2]$  (**1c**) (wire) and of  $[\text{Ni}(\text{dppe})\text{Cl}_2]$  (**I**) (tube) drawn such that the Ni and P atoms from the two structures are coincident. (b) Crystal structures of  $[\text{Ni}(o\text{-MeO-dppe})_2](\text{PF}_6)_2$  (**2e**) (wire) and of  $[\text{Ni}(\text{dppe})_2](\text{NO}_3)_2$  (**II**) (tube) drawn such that the Ni and P atoms from the two structures are coincident (for clarity only one ligand of the bis(chelate) complexes is depicted). (c) Crystal structures of **1c** and of **2e** (for clarity only one ligand is depicted) drawn such that the Ni and P atoms from the two structures are coincident. In all representations the perspective has the depicted P atoms away from the viewer, and the two other not depicted coordinating atoms toward the viewer.

observed before for square-planar  $d^8\text{-ML}_4$  metal complexes.<sup>22</sup> In the crystal packing intermolecular stacking of aryl rings is observed.

**Crystal Structure of  $[\text{Ni}(o\text{-MeO-dppe})_2](\text{PF}_6)_2$  (**2e**).** A molecular drawing of the structure of the complex cation showing 50% probability ellipsoids is given in Figure 3. Selected interatomic distances and angles are given in Table 3. The structure of  $[\text{Ni}(o\text{-MeO-dppe})_2](\text{PF}_6)_2$  (**2e**) resembles that of the related structure of  $[\text{Ni}(\text{dppe})_2](\text{NO}_3)_2$  (**II**).<sup>23</sup> However, the symmetry in **2e** is different from that in **II**. The cation in **II** is centrosymmetric around the nickel(II) center, whereas in the cation of **2e** an exact, crystallographic 2-fold symmetry axis bisecting the ligands is present. In Table 3 the relevant bond distances and angles are compared, whereas in Figure 2b the two compounds are compared in a graphical representation. In both complexes the coordination geometry around the nickel(II) center is essentially square-planar. In the cationic unit of **2e** two aryl rings can be considered to be oriented axially (rings 2 and 3) with respect to the five-membered chelate ring, and two aryl rings are oriented equatorially (rings 1 and 4) as is the case in **II**. However, in the cationic unit of **2e** the axial aryl rings are lying on opposite sides of the five-membered chelate ring, whereas in the cation of **II** the axial phenyl rings are lying on the same side of the five-membered chelate ring, as can be seen in Figure 2b. As in the crystal structure of  $[\text{Ni}(o\text{-MeO-dppe})_2]$ , the *o*-methoxy groups of the axial aryl rings are pointing away from the central nickel atom (torsion angles  $\text{Ni1-P4-C21-C22} = -164.72(13)^\circ$  and  $\text{Ni1-P7-C31-C32} = -170.96(13)^\circ$ ,

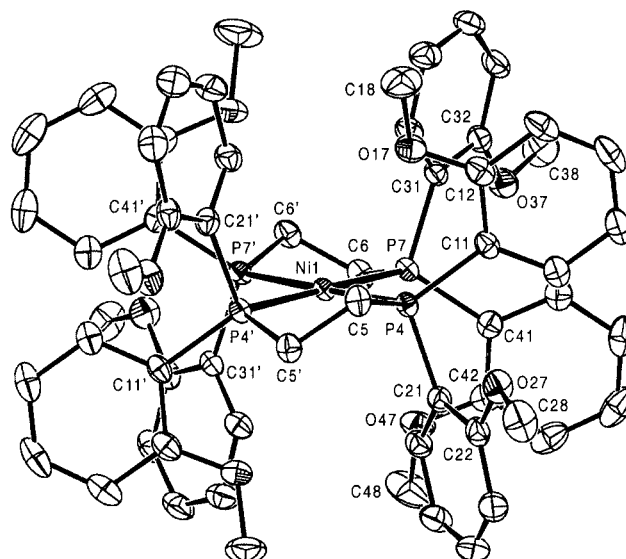


**Figure 3.** Displacement ellipsoid plot (50% probability) of the cationic unit of  $[\text{Ni}(o\text{-MeO-dppe})_2](\text{PF}_6)_2$  (**2e**) with atom-labeling scheme. Hydrogen atoms are omitted for clarity. Symmetry operation:  $1 - x, y, 0.5 - z$ .

whereas the *o*-methoxy groups of the equatorial aryl rings are more pointing toward the nickel atom (torsion angles  $\text{Ni1-P4-C11-C12} = 72.44(14)^\circ$  and  $\text{Ni1-P7-C41-C42} = 74.66(15)^\circ$ ). However, the corresponding  $\text{Ni}\cdots\text{O}$  distances of  $3.9300(14) \text{ \AA}$  (O17) and  $3.9317(14) \text{ \AA}$  (O47) are too large to consider an electrostatic interaction. In Figure 3 it can be seen that the *o*-hydrogen atoms of the axial aryl groups are pointing toward the nickel atom. Again the  $\text{Ni}\cdots\text{H}$  distances of  $2.73 \text{ \AA}$  (H26) and  $2.65 \text{ \AA}$  (H36) indicate the presence of either agostic interactions or  $\text{Ni}\cdots\text{H}-\text{C}$  hydrogen bonds.<sup>22</sup>

**Comparison of the Structures  $[\text{Ni}(o\text{-MeO-dppe})_2]$  (**1c**) and  $[\text{Ni}(o\text{-MeO-dppe})_2](\text{PF}_6)_2$  (**2e**).** In Figure 2c the orientations of the ligands in the structures of **1c** and **2e** are compared. To facilitate the comparison of both structures only one of the ligands in **2e** is shown. It can be seen that in both structures the ligand is oriented in the same way around the central nickel atom, with alternating axial and equatorial orientation of the aryl rings. The ligands in the bis(chelate) complex **2e** are less tightly bound than in the mono(chelate) complex **1c**, which follows from the slightly shorter Ni–P bonds in the latter. The bite angle P–Ni–P in the bis(*o*-MeO-dppe) complex ( $83.34^\circ$ ) is somewhat smaller than the one in the mono(*o*-MeO-dppe) complex ( $86.48^\circ$ ). The steric crowding caused by the presence of two ligands in the coordination sphere of the nickel ion in the bis(*o*-MeO-dppe) complex forces the ligands to adopt a slightly different geometry.

**Characterization of a Mono(chelate) and a Bis(chelate) Complex in Solution.** The chemical shifts in  $^1\text{H}$  NMR and  $^{31}\text{P}\{^1\text{H}\}$  NMR in  $\text{CD}_2\text{Cl}_2$  for the six complexes and the free ligand are summarized in Table 1. The  $^1\text{H}$  NMR spectra in  $\text{CD}_2\text{Cl}_2$  of  $[\text{Ni}(o\text{-MeO-dppe})_2](\text{PF}_6)_2$  (**2e**), as typical for a bis(chelate) complex, and of  $[\text{Ni}(o\text{-MeO-dppe})\text{Cl}_2]$  (**1a**), as typical for a mono(chelate) complex, are shown in Figure 4. The sharp  $^1\text{H}$  NMR signals confirm that the complexes are diamagnetic and that the square-planar geometry around the central nickel atom is retained in solution. This is also observed in the electronic spectra of **1a** and **2e** taken in  $\text{CH}_2\text{Cl}_2$ , which are similar to the diffuse reflectance electronic spectra of the solids. However, as in solution the charge-transfer bands shift to somewhat higher energies, now for **2e** a band at  $29\,600 \text{ cm}^{-1}$  with a shoulder at  $28\,000 \text{ cm}^{-1}$  is observed.

(22) Bouwman, E.; Henderson, R. K.; Powell, A. K.; Reedijk, J.; Smeets, W. J. J.; Spek, A. L.; Veldman, N.; Wocadlo, S. *J. Chem. Soc., Dalton Trans.* **1998**, 3495.

(23) Williams, A. F. *Acta Crystallogr.* **1989**, C45, 1002.



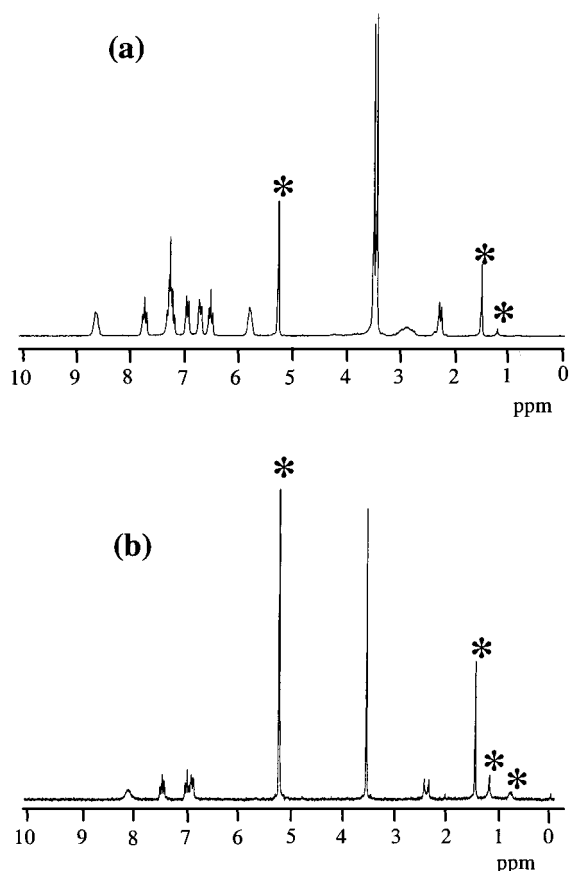
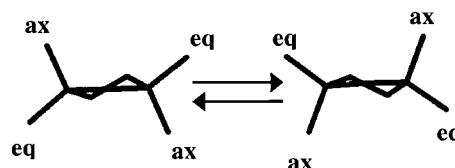


**Figure 4.** (a)  $^1\text{H}$  NMR spectrum of  $[\text{Ni}(\text{o-MeO-dppe})_2](\text{PF}_6)_2$  in  $\text{CD}_2\text{Cl}_2$  at  $25^\circ\text{C}$  as a typical example of a bis(chelate) complex. (b)  $^1\text{H}$  NMR spectrum of  $[\text{Ni}(\text{o-MeO-dppe})\text{Cl}_2]$  in  $\text{CD}_2\text{Cl}_2$  at  $25^\circ\text{C}$  as a typical example of a mono(chelate) complex. Signals arising from solvent or impurities are indicated with an asterisk.

By virtue of the presence of methoxy groups in the ligand, it is possible to distinguish a mono(chelate) complex from a bis(chelate) complex using  $^1\text{H}$  NMR spectroscopy. In the  $^1\text{H}$  NMR spectrum of **2e**, depicted in Figure 4a, eight different signals corresponding to the hydrogen atoms in the aryl groups, two different signals corresponding to the methoxy groups, and two different signals corresponding to the ethylene bridge are observed. This confirms the presence of two types of aryl rings, equatorial and axial, in agreement with the crystal structure of **2e** (see Figure 3). In solution all four equatorial rings are equivalent, as are all four axial rings. The signal corresponding to one type of *o*-hydrogen in **2e** is shifted far downfield to 8.6 ppm. This large downfield shift compared to the free ligand is ascribed to an interaction of the *o*-hydrogen atoms of the axial aryl groups with the filled  $d_{z^2}$  orbital of the nickel atom. This indicates that the short  $\text{Ni}\cdots\text{H}$  distances which are observed in the crystal structure of **2e** are retained in solution. The large downfield shift of these protons in the  $^1\text{H}$  NMR spectrum indicates that the observed  $\text{Ni}\cdots\text{H}$  interaction in the solid state is better described as a hydrogen bond, rather than as an agostic interaction.<sup>24</sup> The signal corresponding to the other type of *o*-hydrogen atom in **2e** is shifted upfield to 5.8 ppm. This large upfield shift is likely to be caused by the shielding of the hydrogen atoms H16 and H46 (connected to C16 and C46, respectively) by the electron clouds of aryl rings 4 and 1, respectively (see Figure 3). At 3.4 and 3.5 ppm signals of the methoxy groups are found, corresponding to the methoxy groups

#### Scheme 4



attached to the axial and to the equatorial aryl rings, respectively. Finally, a doublet at 2.2 ppm and a multiplet at 2.8 ppm corresponding to the ethylene bridge are observed, as the two hydrogen atoms on each of the carbon atoms in the bridge are not equivalent.

In contrast to the complicated  $^1\text{H}$  NMR spectrum of **2e**, the  $^1\text{H}$  NMR spectrum of **1a** is surprisingly simple. In the spectrum depicted in Figure 4b, four different signals corresponding to the hydrogen atoms in the aryl groups, one signal corresponding to the methoxy groups, and one signal corresponding to the ethylene bridge are observed. However, on the basis of the crystal structure of the related compound **1c**, a  $^1\text{H}$  NMR spectrum rather similar to that for **2e** would be expected as also in this compound the four aryl rings are equivalent two by two (see Figure 1 and Figure 2c). The observed spectrum can be explained by assuming the occurrence of a rapid interchange on the NMR time scale of the equatorial and axial aryl groups of two possible rotamers, as depicted in Scheme 4, thus making all four aryl groups of the ligand spectroscopically equivalent. In one rotamer the four aryl groups are arranged as is depicted in Figure 1; in the other rotamer the aryl groups which were oriented axially with respect to the five-membered chelate ring have become equatorial and the equatorial aryl groups have become axial by twisting the ligand about the midpoint of the ethylene bridge while keeping the phosphorus positions fixed. This twist is accompanied by simultaneous rotation of the phenyl groups around the P–C bond, making all four methoxy groups and the *o*-hydrogen atoms mutually equivalent. In the region 6.9–8.1 ppm four signals corresponding to the aryl protons are found. The signal corresponding to the *o*-hydrogens in **1a** is broadened and shifted downfield to 8.1 ppm. This downfield shift is also observed in the  $^1\text{H}$  NMR spectrum of **2e** and can be attributed to an interaction of the *o*-hydrogen atoms of the axial aryl groups with the filled  $d_{z^2}$  orbital of the nickel atom. The downfield shift for **1a** is somewhat smaller than the one observed for **2e**, which can be rationalized with the fluxional behavior of the ligand, leading to a time-averaged signal. Also in the case of **1a** the  $\text{Ni}\cdots\text{H}\cdots\text{C}$  interaction is best described as a hydrogen bond.<sup>24</sup> At 3.6 ppm the signal for the time-average equivalent methoxy groups is observed, and at 2.4 ppm a virtual doublet for the four time-average equivalent hydrogen atoms in the ethylene bridge is present, caused by inequivalent coupling with the two phosphorus atoms.

The differences observed in the NMR spectra of the mono(chelate) and the bis(chelate) are not merely quantitative. It is to be expected that at lower temperatures the NMR spectra of the mono(chelate) complex will show the decoalescence of the signals.<sup>12</sup> Raising the temperature for the bis(chelate) complex does not result in the coalescence of the signals, but instead results in the oxidation of the ligand to the bis(phosphane) oxide. However, in a HH NOESY NMR spectrum exchange peaks were observed, indicating that also the bis(chelate) complex is involved in a dynamic process like the mono(chelate) complex. This process is much faster on the NMR time scale for the mono(chelate) complex than for the bis(chelate) complex due to steric congestion in the latter.

(24) Yao, W.; Eisenstein, O.; Crabtree, R. H. *Inorg. Chim. Acta* **1997**, *254*, 105.

**Table 4.** Summary of the NMR Results in the Study of the Autoionization Equilibrium Using *o*-MeO-dppe. Formation of Mono(ligand) or Bis(ligand) Complexes at 25 °C

	CD <sub>3</sub> OD	acetone- <i>d</i> <sub>6</sub>	CD <sub>2</sub> Cl <sub>2</sub>	acetone- <i>d</i> <sub>6</sub> /toluene- <i>d</i> <sub>8</sub> <sup>a</sup>
[Ni( <i>o</i> -MeO-dppe)Cl <sub>2</sub> ] ( <b>1a</b> )	<i>b</i>	<i>b</i>	mono	<i>c</i>
[Ni( <i>o</i> -MeO-dppe)Br <sub>2</sub> ] ( <b>1b</b> )	<i>b</i>	<i>b</i>	mono	<i>c</i>
[Ni( <i>o</i> -MeO-dppe)I <sub>2</sub> ] ( <b>1c</b> )	<i>b</i>	<i>b</i>	mono	<i>c</i>
[Ni( <i>o</i> -MeO-dppe) <sub>2</sub> ](TFA) <sub>2</sub> ( <b>2d</b> )	bis	<i>c</i>	bis	mono <sup>d</sup>
[Ni( <i>o</i> -MeO-dppe) <sub>2</sub> ](PF <sub>6</sub> ) <sub>2</sub> ( <b>2e</b> )	bis	<i>c</i>	bis	<i>c</i>
[Ni( <i>o</i> -MeO-dppe)(TFA) <sub>2</sub> ] ( <b>1d</b> ) or [Ni( <i>o</i> -MeO-dppe) <sub>2</sub> ][Ni(TFA) <sub>4</sub> ] ( <b>3d</b> )	bis	mono/bis (1:1) <sup>e,f</sup>	mono/bis (3:1) <sup>e</sup>	mono
Ni(OAc) <sub>2</sub> ·4H <sub>2</sub> O: <i>o</i> -MeO-dppe = 1	bis	<i>c</i>	mono	<i>c</i>
Ni(OAc) <sub>2</sub> ·4H <sub>2</sub> O:dppe = 1	bis <sup>g</sup>	<i>c</i>	mono <sup>g</sup>	<i>c</i>

<sup>a</sup> Acetone and toluene were mixed in a 1:4 ratio. <sup>b</sup> Compound is not soluble. <sup>c</sup> Not measured. <sup>d</sup> Free ligand was observed as well. <sup>e</sup> Measured 10 min after the addition of the solvent. <sup>f</sup> This ratio changes to 3:1 after 3 days. <sup>g</sup> Determined using electrospray mass spectroscopy.

For both the mono(chelate) and the bis(chelate) complex only one signal is observed in <sup>31</sup>P{<sup>1</sup>H} NMR, indicating that in each metal complex the phosphorus atoms are equivalent. The difference in chemical shift between free and coordinated ligand, Δδ, is 84–107 ppm, as expected for five-membered chelate rings, which induce a strong deshielding effect.<sup>25</sup> For the TFA compound, it is not possible to assign either a mono(chelate) complex (**1d**) or a bis(chelate) complex (**3d**) using <sup>31</sup>P{<sup>1</sup>H} NMR, as the difference in chemical shift between the two complexes is very small (see Table 1).

**Influence of the Solvent on the Autoionization Equilibrium.** An NMR study of the six complexes was initiated to determine the influence of the polarity of the solvent (methanol ε = 32.6, acetone ε = 20.7, dichloromethane ε = 9.1, and an acetone/toluene mixture ε<sub>toluene</sub> = 2.4)<sup>26</sup> on the nature of the species present in solution. The results of this NMR study are presented in Table 4. For the complexes [Ni(*o*-MeO-dppe)X<sub>2</sub>] (**1**), where X is a strongly coordinating anion (Cl, Br, or I), only the mono(chelate) complex is observed in dichloromethane. Unfortunately, <sup>1</sup>H NMR spectra in methanol and acetone could not be obtained, as these complexes are insoluble in these solvents. The <sup>1</sup>H NMR spectra of these complexes in an acetone/toluene mixture were not taken, as no differences with the spectra obtained in CD<sub>2</sub>Cl<sub>2</sub> are expected. For the complexes [Ni(*o*-MeO-dppe)<sub>2</sub>]Y<sub>2</sub> (**2**), where Y is a more weakly coordinating anion (TFA or PF<sub>6</sub>), only the bis(chelate) complex is observed in dichloromethane, just as in the more polar solvent methanol. In an apolar acetone/toluene (1:4) mixture, the mono(chelate) complex and free, uncoordinated, ligand can be observed; however, the solubility of the complex [Ni(*o*-MeO-dppe)<sub>2</sub>](TFA)<sub>2</sub> (**2d**) in this acetone/toluene mixture is very low.

The intended mono(chelate) complex [Ni(*o*-MeO-dppe)(TFA)<sub>2</sub>] (**1d**) appeared to be the most suitable compound to study the autoionization equilibrium. Upon dissolution of the orange solid in the polar solvent methanol, a yellow solution is obtained, and the typical pattern for a bis(*o*-MeO-dppe) complex is observed. This means that the autoionization equilibrium in this solvent lies completely to the right and the complex is present as **3d**. The <sup>1</sup>H NMR spectrum of an ionized complex appears to be identical to that of a bis(ligand) complex. It seems that the presumably paramagnetic anionic unit of the ionized complex has no influence on the <sup>1</sup>H NMR spectrum of the diamagnetic cationic unit. Upon dissolution of the orange solid in the apolar acetone/toluene mixture, an orange solution is obtained and the typical pattern of a mono(*o*-MeO-dppe) complex is observed, indicating that the equilibrium now lies completely to the left and that the compound is present as **1d**.

Finally, when the orange solid is dissolved in a medium of intermediate polarity (acetone or dichloromethane), a mixture of mono- and bis(chelate) species is observed, whereby the timespan in which equilibrium is reached depends on the solvent used.

In acetone the mono-to-ionized ratio gradually changes in 3 days from 1:1 to 3:1, whereas in dichloromethane a 3:1 ratio is observed instantaneously and this ratio does not change in time. As in acetone the mono-to-ionized ratio gradually changes in favor of the mono(chelate) complex, it is likely that the solid which is initially dissolved largely consists of the ionized complex **3d**. This ionized complex is to some extent stabilized in the more polar solvent acetone and, therefore, more slowly converted to the mono(chelate) complex than in the more apolar dichloromethane.

So, it appears that there is a direct relation between the polarity of the solvent and the position of the autoionization equilibrium. In a polar solvent only the ionized complex is present, whereas in an apolar solvent only the mono(chelate) complex is observed. The influence of the anion on the position of the autoionization equilibrium is discussed below.

**Catalyst Mixtures Containing *o*-MeO-dppe or dppe as the Ligand.** The crystal structure of **2e** and the NMR studies described above show that the presence of the *o*-methoxy group on the phenyl ring does not prevent the formation of an ionized complex. It is of interest to know whether in the in situ prepared mixtures for the catalytic hydrogenation reactions autoionization occurs as well. Therefore, some in situ prepared mixtures, containing nickel(II) acetate and the ligand *o*-MeO-dppe or dppe, were analyzed using both <sup>1</sup>H and <sup>31</sup>P{<sup>1</sup>H} NMR spectroscopy (see Table 4). As the mono(dppe) and bis(dppe) complexes cannot readily be distinguished using NMR spectroscopy, the nature of the species present in solution was determined using electrospray mass analysis. In methanol, the solvent that is used in the reported catalytic hydrogenation experiments,<sup>8</sup> only the ionized complex is observed for both ligands, whereas in dichloromethane only the mono(chelate) complex proved to be present in both cases. This result indicates that, apart from the solvent, also the anion has a considerable influence on the position of the autoionization equilibrium as for the TFA complex **1d** in chloroform a mixture of mono- and bis(chelate) species is present. The stronger are the coordinating abilities of the anion, the more the autoionization equilibrium will be shifted toward the mono(chelate) complex in a solvent of intermediate polarity.

In the case of *o*-MeO-dppe the influence of methanol on the autoionization equilibrium was investigated. Even when only 5 drops (~2%) of CD<sub>3</sub>OD were added to a solution of nickel(II) acetate and the ligand in CD<sub>2</sub>Cl<sub>2</sub>, approximately 30% of the mono(chelate) complex was converted to the ionized complex

(25) Garrou, P. E. *Chem. Rev.* **1981**, *81*, 229.

(26) Burger, K. *Organic Reagents in Metal Analysis*; Pergamon Press: Oxford, 1973; Table 59.



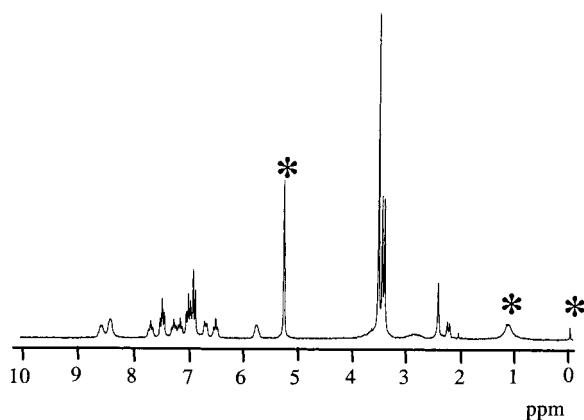


**Figure 5.**  $^1\text{H}$  NMR spectrum of nickel(II) acetate mixed with *o*-MeO-dppe (1:1) in  $\text{CD}_2\text{Cl}_2$  at  $25\text{ }^\circ\text{C}$  after the addition of 5 drops of  $\text{CD}_3\text{OD}$ . Signals arising from solvent or impurities are indicated with an asterisk.

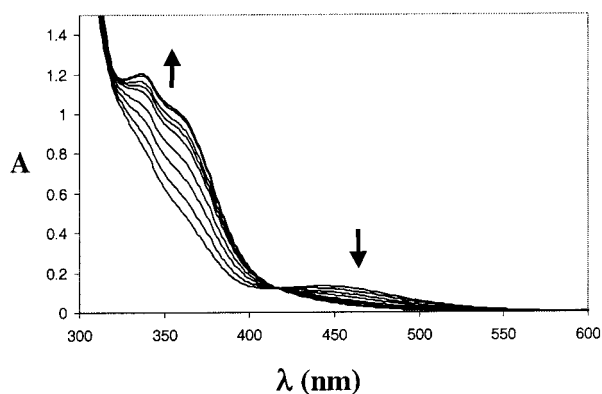


**Figure 6.** Electronic absorption spectra of the in situ formed complex using  $\text{Ni}(\text{OAc})_2 \cdot 4\text{H}_2\text{O}$  and *o*-MeO-dppe (1:1) in a dichloromethane/methanol mixture (4:1) recorded at  $25\text{ }^\circ\text{C}$  under Ar. Spectra recorded during 3 h after dissolution, at 3, 5, 10, 15, 30, 45, 60, 120, and 180 minutes.

(see Figure 5).<sup>27</sup> In a 1:1 mixture of methanol and dichloromethane, which appeared to be the most suitable for catalytic hydrogenation reactions,<sup>28</sup> only the ionized complex can be observed in NMR.

**Some Aspects of the Autoionization Equilibrium.** Electronic absorption spectroscopy was used to prove that the mono(chelate) complex is converted to the bis(chelate) complex in the autoionization equilibrium. When *o*-MeO-dppe and nickel(II) acetate are mixed in a 1:1 ratio in a 4:1 mixture of dichloromethane and methanol, the conversion of mono(chelate) complex into ionized complex can be followed in time, as is shown in Figure 6. In 2 h the absorption at 450 nm, corresponding to the mono(chelate) complex, disappears, while an absorption at 340 nm and a shoulder at 360 nm, corresponding to the bis(chelate) complex, appear after 15 min and increase in intensity with time. An isosbestic point is observed at 420 nm, indicating that one species is converted into the other, and the color of the solution slowly changes from orange to yellow.

The question arises whether the ionized complex can be reconverted to the mono(chelate) complex. Therefore, an ionized complex was generated using nickel(II) acetate and *o*-MeO-

**Table 5.**  $^{31}\text{P}\{^1\text{H}\}$  NMR Data (recorded at  $25\text{ }^\circ\text{C}$ ) of the Experiments Mimicking the Catalytic Conditions Using *o*-MeO-dppe and dppe as the Ligands

	<i>o</i> -MeO-dppe	dppe
$\text{Ni}(\text{OAc})_2 \cdot 4\text{H}_2\text{O}:\text{ligand} = 1:1$	52.5 (s)	54.4 (s)
in $\text{CD}_3\text{OD}$		
+ 1 h at $50\text{ }^\circ\text{C}$	52.5 (s)	54.4 (s), 34.6 (s)
		(ratio 1:2)
+ 10 bar of $\text{H}_2$ pressure	53.5 (s)	55.4 (s)
+ 10 bar of $\text{H}_2$ pressure and	53.5 (s)	55.3 (s), 35.4 (s)
30 min at $50\text{ }^\circ\text{C}$		(ratio 1:1)
spent catalyst in $\text{CD}_3\text{OD}$	52.5 (s)	<i>a</i>

<sup>a</sup> Not measured.

dppe (in a 1:1 ratio) in methanol. Subsequently, the solvent was evaporated and the remaining solid was dissolved in dichloromethane. It appeared that the ionized complex was indeed converted to the mono(*o*-MeO-dppe) complex, as indicated by  $^1\text{H}$  NMR spectroscopy. From these experiments it appears that the autoionization equilibrium is fully reversible.

The identity of the anionic part of the ionized complex (**3**) was investigated by electrospray mass spectroscopy in the negative mode. Electrospray mass analysis of the in situ formed complex using  $\text{Ni}(\text{OAc})_2 \cdot 4\text{H}_2\text{O}$  and *o*-MeO-dppe in methanol showed the presence of  $\text{OAc}^-$ ,  $[\text{Ni}(\text{OAc})_3]^-$ , and a very small amount of  $[\text{Ni}_2(\text{OAc})_5]^-$ . In view of these findings it is probably more correct to represent the ionized complex (**3**) as  $[\text{Ni}(\text{o-MeO-dppe})_2][\text{Ni}(\text{OAc})_3](\text{OAc})$ .

**Probing the Working Hypothesis.** From the studies described above it appears that the differences in catalytic hydrogenation activity of nickel(II) acetate in combination with dppe or *o*-MeO-dppe cannot be rationalized by the autoionization hypothesis. Therefore, in situ prepared catalytic mixtures containing nickel(II) acetate and either of these ligands were further studied in order to try to get some insight into the origin of the positive effect of the *o*-methoxy group on the catalytic activity. The catalyst, nickel(II) acetate and the ligand dissolved in methanol, was heated to  $50\text{ }^\circ\text{C}$  under dihydrogen pressure of 10 bar and analyzed using  $^{31}\text{P}\{^1\text{H}\}$  NMR spectroscopy. The results are presented in Table 5. Under all conditions in the case of *o*-MeO-dppe only the ionized complex was observed, also in a spent catalyst after a catalytic hydrogenation reaction. However, in the  $^{31}\text{P}\{^1\text{H}\}$  NMR spectra of the solutions containing the ligand dppe in some cases a peak at 34.6 ppm appears besides the peak at 54.4 ppm. LC-MS analysis showed the peak at 34.6 ppm to originate from the fully oxidized dppe ligand [bis(phosphane oxide)]. This signal appears when the solution is heated, even under reducing conditions, indicating that the dppe ligand is oxidized under the catalytic hydrogenation conditions.

**New Hypothesis.** Oxidation of the ligand may account for the difference in activity between catalysts containing the ligands *o*-MeO-dppe and dppe. This oxidation was expected to be an important factor in the case of complexes containing the ligands *o*-MeO-dppp and dppp, as with these ligands autoionization to bis(chelate) complexes is not observed at all.<sup>12</sup> Therefore, the spent catalyst after a hydrogenation reaction, employing a catalyst based on either of the two ligands, was analyzed using  $^{31}\text{P}\{^1\text{H}\}$  NMR spectroscopy. In the case of *o*-MeO-dppp no oxidized ligand was observed, whereas dppp was oxidized to the bis(phosphane oxide). Monitoring the fate of dppp in  $\text{CDCl}_3$  at room temperature, it appeared that ligand is fully oxidized in 6 h in the presence of nickel(II) acetate, whereas in the absence of nickel(II) acetate the ligand is hardly oxidized over the same period of time. Moreover, as all experiments were

(27) Surprisingly, the NMR spectra do not show the presence of the acetate anions. In the case of a bis(chelate) complex this can be explained by the formation of paramagnetic  $[\text{Ni}(\text{OAc})_3]^-$  or  $[\text{Ni}(\text{OAc})_4]^{2-}$  species, which are not visible in the NMR. In the case of mono(chelate) complexes we assume that this is caused by intermediate exchange of the coordinating acetate ions with the methanol solvent.

(28) Angulo, I. M.; Bouwman, E.; Lok, S. M.; Quiroga, V. F. In preparation.

carried out in an inert atmosphere the oxidation seems to be related to the nickel(II) center, as already observed by Jarrett et al.<sup>10</sup> It was reported earlier that Pd(OAc)<sub>2</sub> is able to oxidize tertiary phosphanes.<sup>29</sup> We now believe that in our case also the Ni(OAc)<sub>2</sub> oxidizes the tertiary phosphane ligands dppe and dppp, whereas the ligands *o*-MeO-dppe and *o*-MeO-dppp are not oxidized.

Prevention of oxidation of the phosphorus atom by the *o*-methoxy group could again be due to either a steric or electronic effect. We have reported<sup>8</sup> that when using *p*-MeO-dppp<sup>9</sup> no catalytic hydrogenation activity is observed. <sup>31</sup>P{<sup>1</sup>H} NMR spectroscopy shows that also in this case the ligand is rapidly oxidized. These two observations imply that the prevention of oxidation in the *o*-methoxy-substituted ligands is merely steric; the nearby presence of an *o*-methoxy group shields the phosphorus atom to which it is attached from oxidation.

### Conclusion

It has become clear that the *o*-methoxy substituent on the phenyl groups in the ligand *o*-MeO-dppe does not prevent autoionization of the nickel complexes coordinated by this ligand. In a polar solvent in combination with weakly coordinating anions—the conditions used in the catalytic hydrogenation of 1-octene—only the ionized complex is observed, whereas in an apolar solvent in combination with coordinating anions only the mono(chelate) complex occurs. Complexes containing the ligands *o*-MeO-dppp and dppp do not show autoionization to bis(chelate) complexes.<sup>12</sup> It is shown that the role of the methoxy substituents in *o*-MeO-dppe and *o*-MeO-dppp may be that these prevent oxidation of the ligand. This oxidation appeared to be rapid in the case of the unsubstituted ligands dppe and dppp, whereas it is relatively slow or nonexistent for *o*-MeO-dppe and *o*-MeO-dppp.

Although the *o*-methoxy groups in *o*-MeO-dppe do not prevent autoionization, still the derived nickel complexes yield active hydrogenation catalysts. The performance of the *o*-MeO-dppe containing nickel(II) catalysts is rather sensitive toward variations in solvents and anions, which is presumably due to the occurrence of the autoionization equilibrium.<sup>28</sup> The catalytic activity of this system may (partly) be explained by the presence of the apolar substrate 1-octene. The addition of this apolar substrate in a significant amount will lower the overall polarity of the reaction mixture and thereby will shift the autoionization equilibrium in favor of the mono(chelate) complex. As the nickel complexes containing the ligand *o*-MeO-dppe are involved in an autoionization equilibrium under the conditions used in catalytic hydrogenation reactions, it may well be that only a small part of the available nickel complexes is involved in hydrogenation catalysis. It is expected that when autoionization could be suppressed, more active hydrogenation catalysts are to be obtained.

**Acknowledgment.** This research has been financially supported by the Council for Chemical Science of the Netherlands Organization for Scientific Research (CW-NWO). We thank Dr. J. Reedijk and Dr. E. Drent for fruitful discussions. We thank A. B. van Oort (Shell) for measuring the high-pressure NMR spectra, Dr. W. Genuit (Shell) for measuring MS and LC-MS spectra, and V. F. Quiroga (Leiden) for measuring electronic absorption spectra.

**Supporting Information Available:** X-ray crystallographic files in CIF format for the complexes [Ni(*o*-MeO-dppe)<sub>2</sub>] and [Ni(*o*-MeO-dppp)<sub>2</sub>](PF<sub>6</sub>)<sub>2</sub>. This material is available free of charge via the Internet at <http://pubs.acs.org>.

(29) Amatore, C.; Carré, E.; Jutand, A.; M'Barki, M. A. *Organometallics* **1995**, *14*, 1818.